Supplementary Information (SI) for Inorganic Chemistry Frontiers.

Continuous Energy-Level Distribution of $Zn_XCd_{1-X}S$ Induced by Gradient Oxygen Doping for Efficient Photoelectrochemical Water Splitting

Kunpeng Wang, [†a] Xinyu Hu, [†a] Yuxin Yao, [a] Jiafang Liu [*a] and Shikuo Li [*a]

[a]School of Materials Science and Engineering, Key Laboratory of Structure and Functional Regulation of Hybrid Materials of Ministry of Education, Anhui University, Hefei, 230601, P. R. China

†: Kunpeng Wang and Xinyu Hu contributed equally to this work

Corresponding author.

E-mail addresses: lishikuo@ahu.edu.cn, ljf199791@mail.ustc.edu.cn;

1. Experiment Section

1.1 Characterizations.

The morphology of the samples was characterized by scanning electron microscopy (SEM, Sigma 500, Germany). Transmission electron microscopy and high-resolution transmission electron microscopy (TEM/HRTEM, JEM-2100, Japan) were used to examine the microstructure and lattice features. X-ray diffraction (XRD) patterns were recorded using an X-ray diffractometer (SmartLab 9 kW, Japan). The surface chemical states were analyzed by X-ray photoelectron spectroscopy (XPS, ESCALAB 250Xi, USA). Room-temperature photoluminescence (PL) spectra were collected using an FS5 fluorescence spectrometer (Edinburgh Instruments, UK). Raman spectra were obtained using a confocal Raman spectrometer (inVia-Reflex, UK) at room temperature.

1.2 Photoelectrochemical (PEC) performance measurements.

PEC measurements were carried out on an electrochemical workstation (CHI 760e, CH Instruments Inc., China) at room temperature with a conventional three-electrode cell. The prepared photoanode with an exposed area of 1cm^2 was employed as the working electrode, while the saturated Ag/AgCl electrode and Pt foil were used as the reference electrode and counter electrode, respectively. A 300 W xenon arc lamp (CEL-PE300L-3A) with a filter (AM 1.5 G, Ceaulight Technology Co. Ltd., China) was employed to simulate solar illumination with about 1 Sun power. The back-side illumination through the FTO side was adopted for all the PEC tests.[1] The photo-oxidation of sulfite performance was measured in a 0.35M Na_2SO_3 and 0.25M Na_2S-mixed solution (pH = 12.5), while the photo-oxidation of water performance was measured in a 0.5M Na_2SO_4 solution (pH = 7). To study the kinetics of charge transfer and recombination, 0.5M Na_2SO_4 solution (pH = 7) was used as the electrolyte. During the evaluation of the PEC performance, all measured potentials were converted to reversible hydrogen electrode (RHE) using the Nernst equation below.

The IPCE was calculated from the equation:

$$\mathrm{IPCE} = [\frac{1024 \times J(mAcm^{-2})}{\lambda(nm) I_{light}(mWcm^{-2})}] \times 100\% \quad \text{(S1)}$$

where, λ is the incident light wavelength, J is the photocurrent density at wavelength λ under illumination, and Ilight is the incident light irradiance intensity.

The built-in electric field strength (E_b) can be calculated according to the following formula:

$$E_b = [\frac{-2V_s\rho}{\varepsilon\varepsilon_0}]^{1/2} \quad \text{(S2)}$$

where, E_b is the built-in electric field intensity, Vs is the surface photovoltage, ρ is the surface charge density, ε is the low frequency dielectric constant, and ε_0 is the dielectric constant in free space. The surface charge density can be obtained by integrating the peak value of transient anodic current.[2]

1.3 Theoretical calculations

The Vienna Ab Initio Package (VASP) was employed to perform all the density functional theory (DFT) calculations within the generalized gradient approximation (GGA) using the Perdew, Burke, and Enzerhof (PBE) formulation.[3-5] The projected augmented wave (PAW) potentials were applied to describe the ionic cores and take valence electrons into account using a plane wave basis set with a kinetic energy cutoff of 500 eV,[6, 7] A vacuum layer of 15 Å was established to avoid interlayer effects. Under standard conditions, the Gibbs free energy (ΔG) of the OER reaction can be calculated according to the following formula:

$$G = E + E_{ZPE} - TS - eU \tag{S3}$$

where E, E_{ZPE}, and S represent the single-point energy, zero-point energy, and entropy of the ZCS, and O-ZCS, respectively, with and without different oxygen intermediates adsorbed. T indicates a temperature of 298.15 K. U is the potential compared to a typical hydrogen electrode.

For the oxygen evolution reaction, we considered the four elementary steps:

$$H_2O + * \rightarrow OH* + H^+ + e^- \tag{S4}$$

$$OH* \rightarrow O* + H^+ + e^- \tag{S5}$$

$$O* + H_2O \rightarrow OOH* + H^+ + e^- \tag{S6}$$

$$OOH* \rightarrow * + O_2 \uparrow + H^+ + e^- \tag{S7}$$

where * represents a surface site and *OH, *O, and *OOH are intermediates adsorbed on an active site on the catalyst surface.

The overpotential (η) are calculated as follows:

$$\eta = \frac{\max\{\Delta G_1, \Delta G_2, \Delta G_3, \Delta G_4\}}{e} - 1.23 \tag{S8}$$

Here, ΔG1, ΔG2, ΔG3, and ΔG4 denote the Gibbs free energy difference for each reaction, (S4)-(S7), respectively.

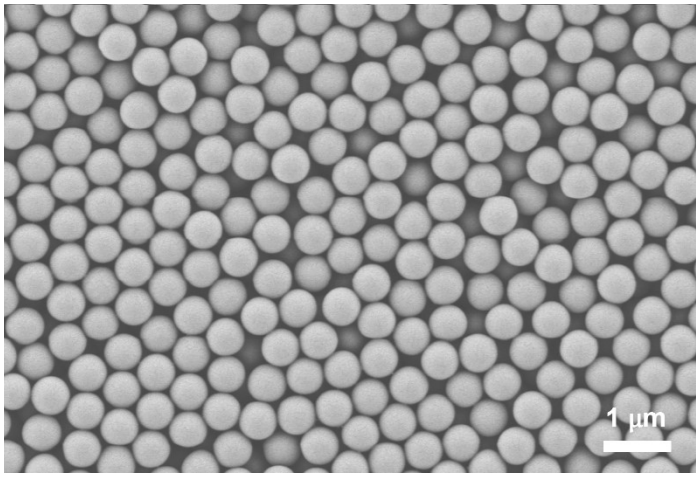

Figure S1. The SEM image of the three-dimensional ordered polystyrene sphere template.

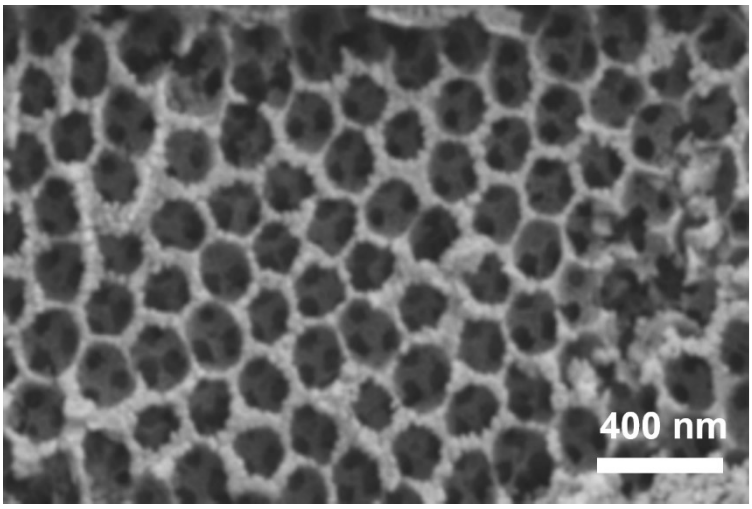

Figure S2. The SEM image of the ZnO photonic crystal.

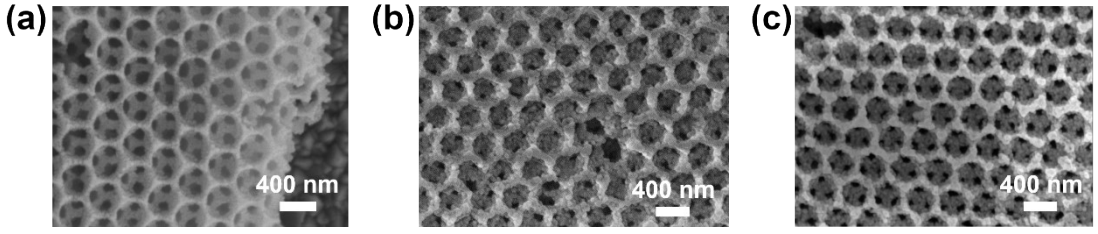

Figure S3. The SEM images of O-ZCS samples after heat treatment at (a) 400 °C, (b) 450 °C, and (c) 600 °C.

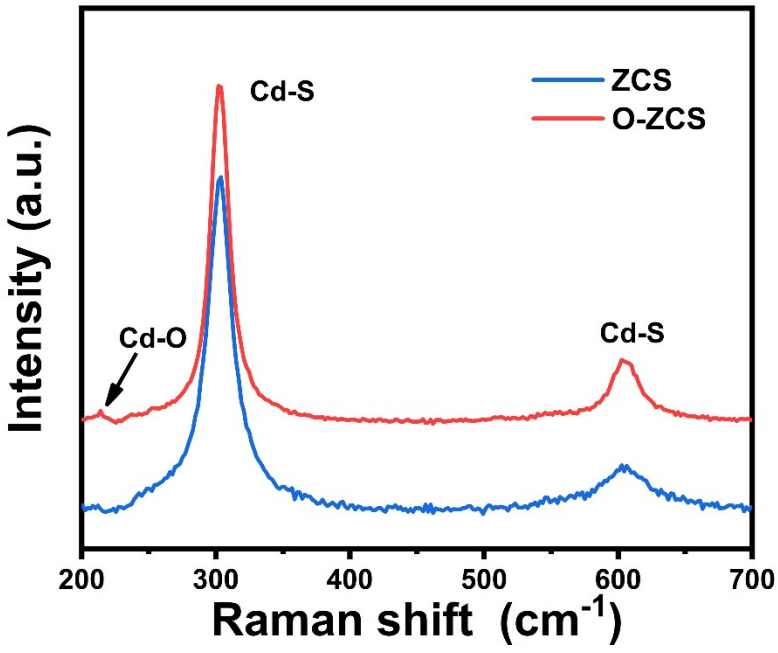

Figure S4. The Raman spectra of ZCS and O-ZCS samples.

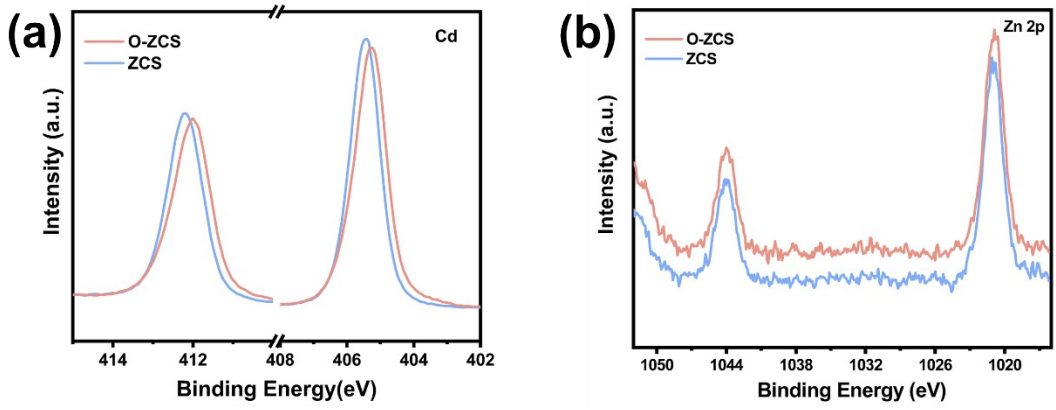

Figure S5. High-resolution XPS spectra of (a) Cd 3d and (b) Zn 2p for the O-ZCS sample.

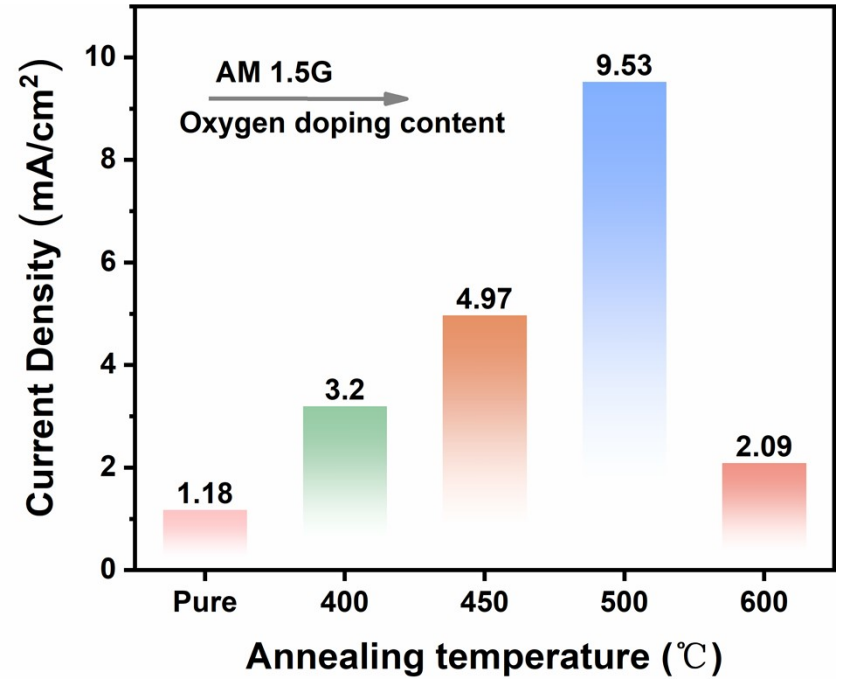

Figure S6. The photocurrent density of a series of O-ZCS samples at different annealing temperatures.

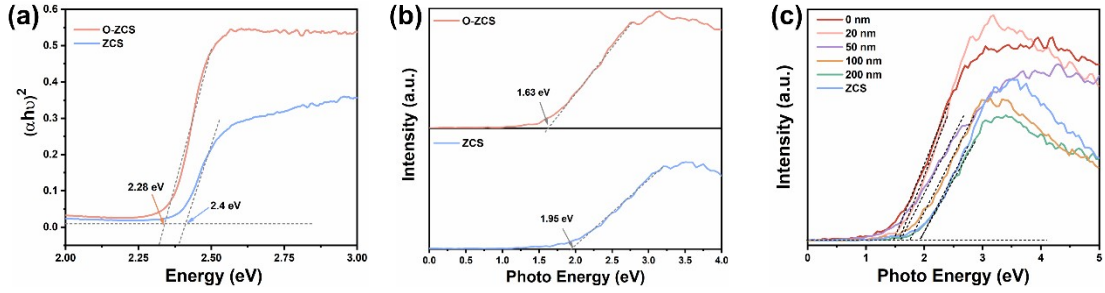

Figure S7. (a) The plot of $(ahν)^2$ *vs* hν of the ZCS and O-ZCS photoanodes; (b) the UPS valence-band spectrum of ZCS and O-ZCS photoanodes; (c) the UPS valence band spectra of O-ZCS sample at different etching depths.

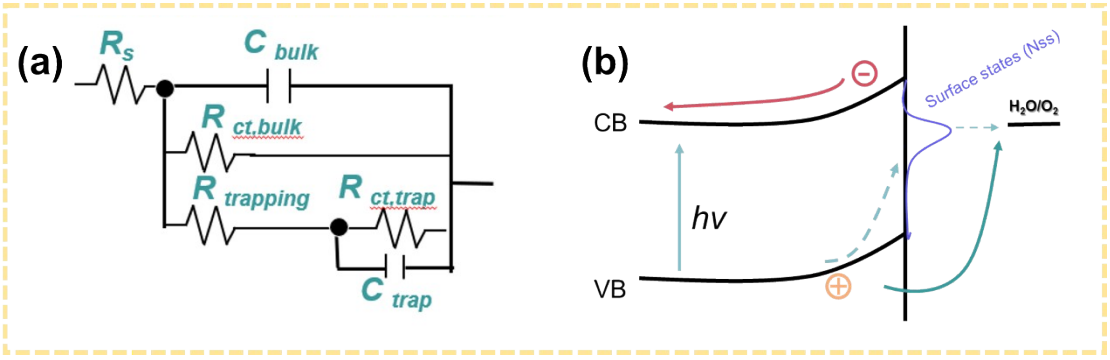

Figure S8. (a) Equivalent circuit used for PEIS fitting. (b) Schematic model of hole transfer at the O-ZCS photoanode surface without an auxiliary catalyst.

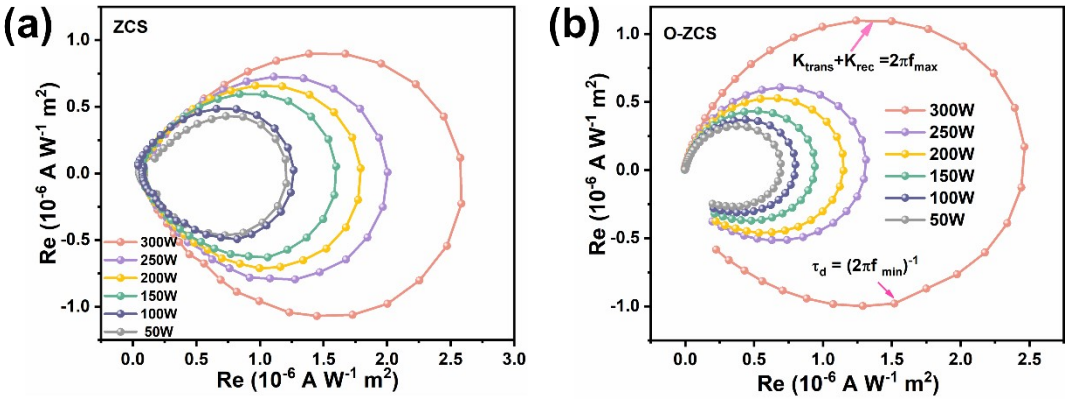

Figure S9. IMPS spectra of (a) O-ZCS and (b) ZCS photoanodes.

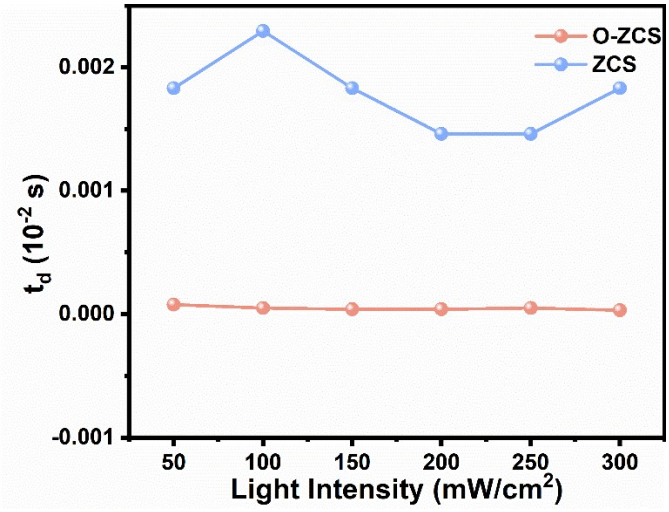

Figure S10. Charge transfer rates of ZCS and O-ZCS photoanodes.

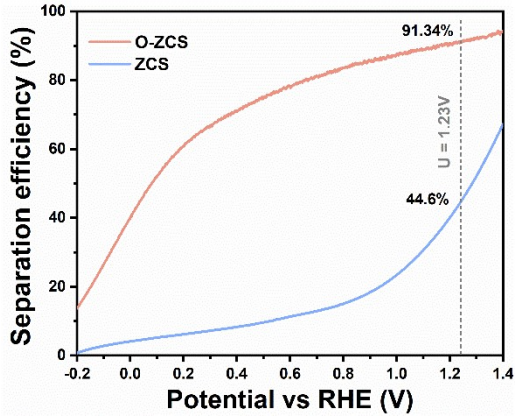

Figure S11. Curves of ZCS and O-ZCS bulk phase charge separation.

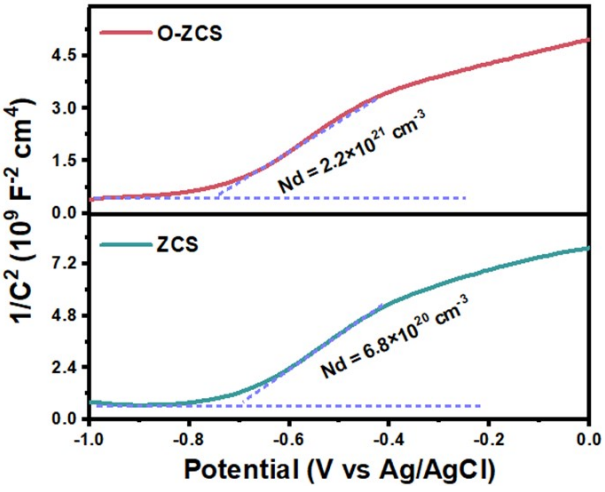

Figure S12. Mott-Schottky curves of ZCS and O-ZCS.

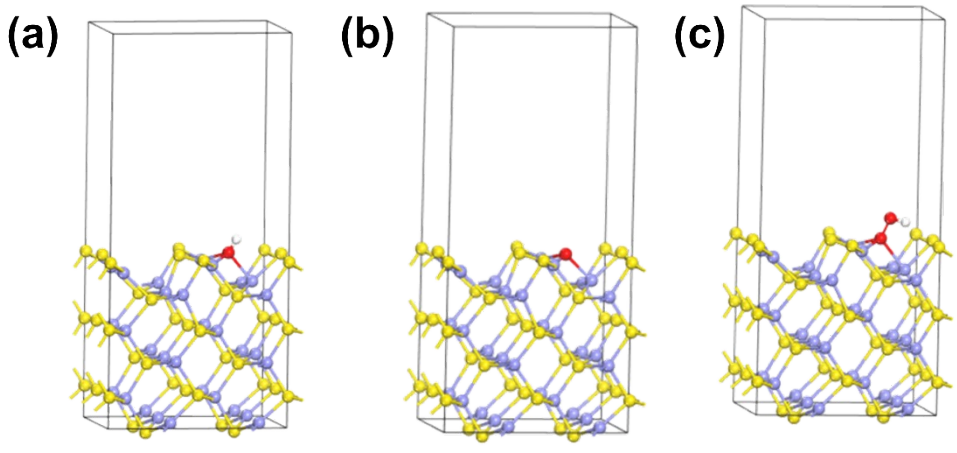

Figure S13. Optimized adsorption configurations of OH* (a), O* (b), and OOH* (c) intermediates on ZCS .

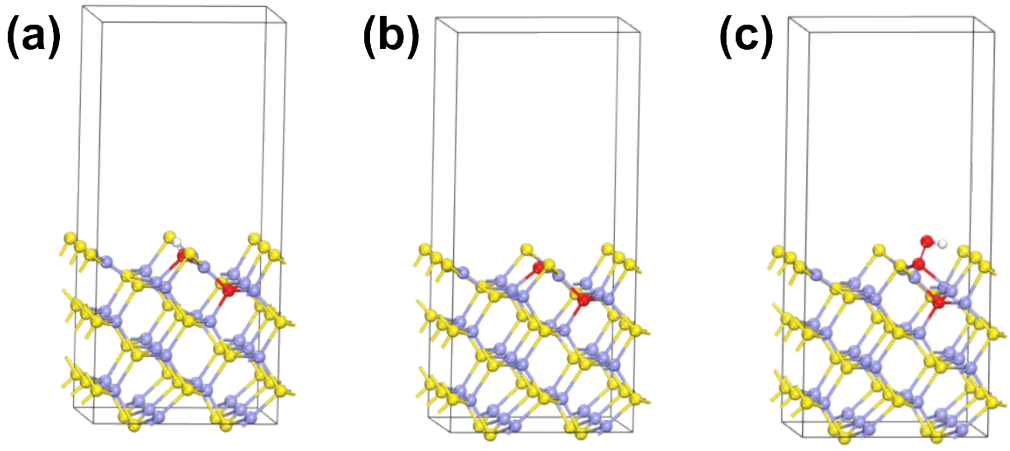

Figure S14. Optimized adsorption configurations of OH* (a), O* (b), and OOH* (c) intermediates on O-ZCS.

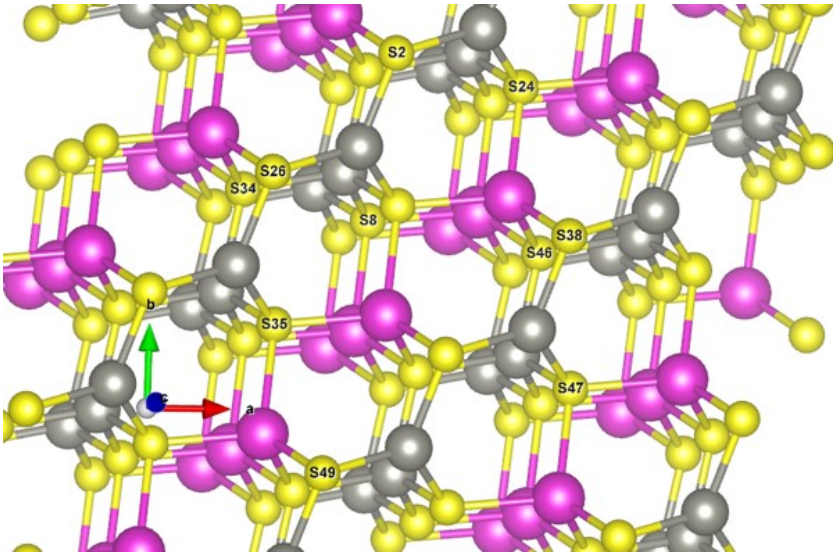

Figure S15. The localized enlarged image of the ZCS crystal model.

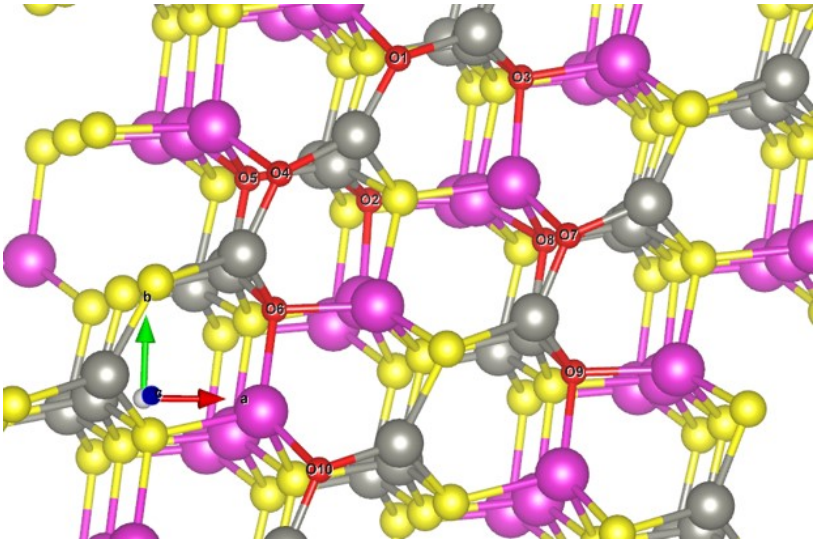

Figure S16. The localized enlarged image of the O-ZCS crystal model.

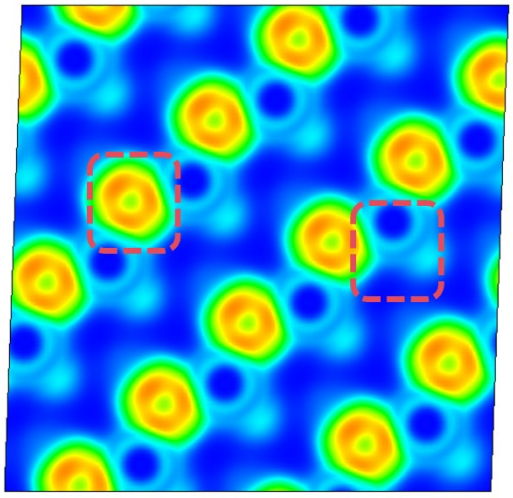

Figure S17. Localized electron distribution of ZCS.

References

[1] Zhang, S.; Lie, S.; Chen, Y.; Chun, H. Z.; Ahmed, M. G.; Sadhu, A.; Sun, Q.; Julianto, E.; Salim, T.; Yuwono, A. H.; Wong, L. H. Efficient hydrogen generation by photoelectrochemical water splitting using Cu_2CdSnS_4 photocathode. Chem. Eng. J. 2026, **527**, 171647.

[2] Yu, W.; Feng, C.; Li, R.; Zhang, B.; Li, Y. Recent advances in tantalum nitride for photoelectrochemical water splitting. Chin. J. Catal. 2025, **68**, 51-82.

[3] Furthmüller, J.; Kresse, G. Efficient iterative schemes for ab initio total-energy calculations using a plane-wave basis set. Phys. Rev. B 1996, **54**, 11169-11186.

[4] Burke, K.; Ernzerhof, M.; Perdew, J. P. Generalized gradient approximation made simple. Phys. Rev. Lett. 1996, **77**, 3865-3868.

[5] Joubert, D.; Kresse, G. From ultrasoft pseudopotentials to the projector augmented-wave method. Phys. Rev. B 1999, **59**, 1758-1775.

[6] Blöchl, P. E. Projector augmented-wave method. Phys. Rev. B 1994, **50**, 17953-17979.

[7] Grimme, S.; Antony, J.; Ehrlich, S.; Krieg, H. A consistent and accurate ab initio parametrization of density functional dispersion correction (DFT-D) for the 94 elements H-Pu. J. Chem. Phys. 2010, **132**, 154104.